Acta Oceanologica Sinica 2009, Vol.28, No.4, p.1-7
http://www.hyxb.org.cn
E-mail: hyxbe@263.net

Three-dimensional structure of a low salinity tongue in the southern Taiwan Strait observed in the summer of 2005

HONG Huasheng[1], ZHENG Quanan[2], HU Jianyu[1]*, CHEN Zhaozhang[1], LI Chunyan[3], JIANG Yuwu[1], WAN Zhenwen[1]

[1] State Key Laboratory of Marine Environmental Science, College of Oceanography and Environmental Science, Xiamen University, Xiamen 361005, China

[2] Department of Atmospheric and Oceanic Science, University of Maryland, College Park, MD 20742, USA

[3] Department of Oceanography and Coastal Sciences, Coastal Sciences, School of the Coast and Environment, Louisiana State University, Baton Rouge, LA 70803, USA

Received 9 April 2008; accepted 8 February 2009

Abstract
Cruise observations with CTD (conductivity-temperature-depth) profiler were carried out in the southern Taiwan Strait in the summer of 2005. Using the cruise data, two-dimensional maps of salinity and temperature distributions at depths of 5, 10, 15, 20, and 30 m were generated. The maps show a low salinity tongue sandwiched by low temperature and high salinity waters on the shallow water side and high temperature and high salinity waters on the deep water side. The further analysis indicates that the low salinity water has a nature of river-diluted water. A possible source of the diluted water is the Zhujiang (Pearl) Estuary. Meanwhile, the summer monsoon is judged as a possible driving force for this northeastward jet-like current. The coastal upwelling and the South China Sea Warm Current confine the low salinity water to flow along the central line of the strait. Previous investigations and a numerical model are used to verify that the upstream of the low salinity current is the Zhujiang Estuary. Thus, the low salinity tongue is produced by four major elements: Zhujinag Estuary diluted water, monsoon wind driving, coastal upwelling and South China Sea Warm Current modifications.

Key words: Taiwan Strait, low salinity tongue, river diluted water, cruise measurement

1 Introduction

The Taiwan Strait is a channel for the water exchange between the East China Sea and the South China Sea (SCS). Various circulation systems (Bao et al., 2005; He et al., 2002; Liu and Yuan, 1999) meet in this narrow strait and are modified by complicated bottom topography, so that complex circulation patterns are produced there. The tides in the Taiwan Strait are generated by the Pacific tidal waves, which enter the strait through both southern and northern entrances and converge in the middle strait (Ding, 1983; Jan et al., 2004; Chen, 1983; Chen et al., 1999). A generally accepted concept, though it is still a controversy, is that the circulation in the Taiwan Strait consists of two major subsystems. On the southern and eastern sides of the strait, the SCS Warm Current flows northeastward along the shelf break of northern SCS (Guan and Fang, 2006; Li et al., 2000) and then turns northward through the Penghu Channel all the year round (Chuang, 1986). On the western side, a seasonally varying coastal current is modulated by the annual cycle of monsoon wind forcing (Kuo and Ho, 2004). Particularly in winter, the northeasterly monsoon wind drives a narrow southward Zhejiang-Fujian Coastal Current (Zheng and Klemas, 1982). In summer, the southwesterly wind drives coastal upwelling with strong fronts (Hu et al., 2001b, 2003; Li et al., 2000). These previous results have addressed general features of the circulation in the Taiwan Strait.

Foundation item: This study was supported by the National Natural Science Foundation of China under contract Nos 40331004, 40576015, 40810069004 and 40821063, the MEL Open Project MEL0506, and partially supported by the ONR through grants N00014-05-1-0328 and N00014-05-1-0606, and the NSF through Grant 071003-9222 (for Zheng, any opinions, findings, and conclusions or recommendations expressed in this paper are those of the authors and do not necessarily reflect the views of the NSF).
*Corresponding author, E-mail: hujy@xmu.edu.cn

However, the fine structure of the circulation still remains unclear due to the lack of the field work.

Since the 1990s, cruise observation activities in the Taiwan Strait have been intensified. In 1994, a joint cruise program was conducted in the southern Taiwan Strait (Hu et al., 1999; Li et al., 1998). In the summer of 2000, the underway observations of sea surface temperature (SST) and salinity were carried out (Zhuang et al., 2003). In the summer of 2005, cruise observations were repeated in the same survey area. The CTD (conductivity-temperature-depth) data obtained by this cruise will be analyzed in this paper.

2 Cruise observations

The cruise was carried out by R/V *Yanping No.2* from 4 to 15 July 2005 (Chen et al., 2005). As shown in Fig. 1, the survey area covers a rectangular region of 130 km by 160 km, which is enclosed by the lines linking four points from A1 (23.63°N, 117.85°E) clockwise in turn to A9 (22.53°N, 118.92°E), C9 (21.67°N, 117.91°E), and C1 (22.79°N, 116.77°E). The water depth varies from 25 to 500 m. The cruise underway observations of sea surface temperature and salinity conducted in the summer of 2000 have revealed the complex frontal structure in the surface layer of this region (Zhuang et al., 2003). Unfortunately, the lower layer structure remains unclear. Thus, this cruise aims to collect the temperature and salinity profile data and to use the data for further understanding the three-dimensional (3-D) fine structure of the circulation. During the cruise observation, the survey area was mapped by CTD casts at 55 stations along five cross-shelf transects. The horizontal resolution of observation grids is about 20 km by 35 km. At each station, the data were measured continuously from the surface to the depth near bottom with a vertical resolution of 1 m.

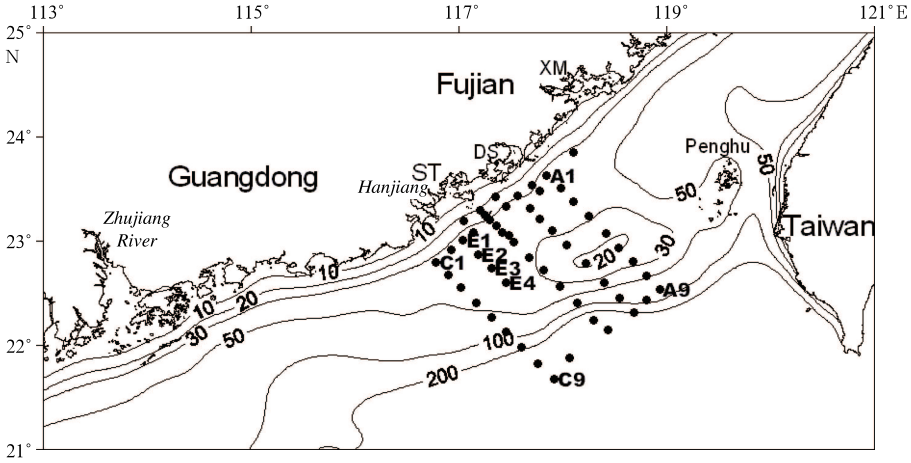

Fig.1. A map of the survey area. Codes represent CTD cast stations. Numerals on isobaths are in m. In the figure, ST, DS and XM represent Shantou, Dongshan and Xiamen, respectively.

Figure 2 shows examples of temperature and salinity profiles measured at Stas E1, E2, E3 and E4 (see Fig. 1 for locations), which are located at a cross-shore section. One can see the fine structure of vertical stratification. The ocean is characterized by two layers: an upper layer with a depth of 5–15 m, which has a high temperature (29.5°C at Sta. E1 or 30.5°C at Sta. E3) and a low salinity (27.0 at Sta. E1 or 31.7 at Sta. E3), and a lower layer below 25 m depth having a low temperature (21.5°C at Sta. E1 or 22.8°C at Sta. E3) and a high salinity (34.6 at each station). There is a sharp thermocline between the two layers. The temperature gradient reaches as high as 1°C/m at the nearshore stations (E1 and E2), implying that these nearshore stations are located in a frontal zone of coastal current.

3 Cruise data analysis

Using the cruise data and interpolation methods (Hu et al., 2001a), two-dimensional (2–D) distribution maps of the salinity at depths of 5, 10, 15, 20, and 30 m are generated as shown in Figs 3a–e. One can see that the most remarkable feature shown in Figs 3a and b is a low salinity tongue sandwiched by high salinity waters on both shallow and deep water sides. The low salinity tongue runs southwest–northeastward along 40–50 m isobaths. The tongue axis is generally

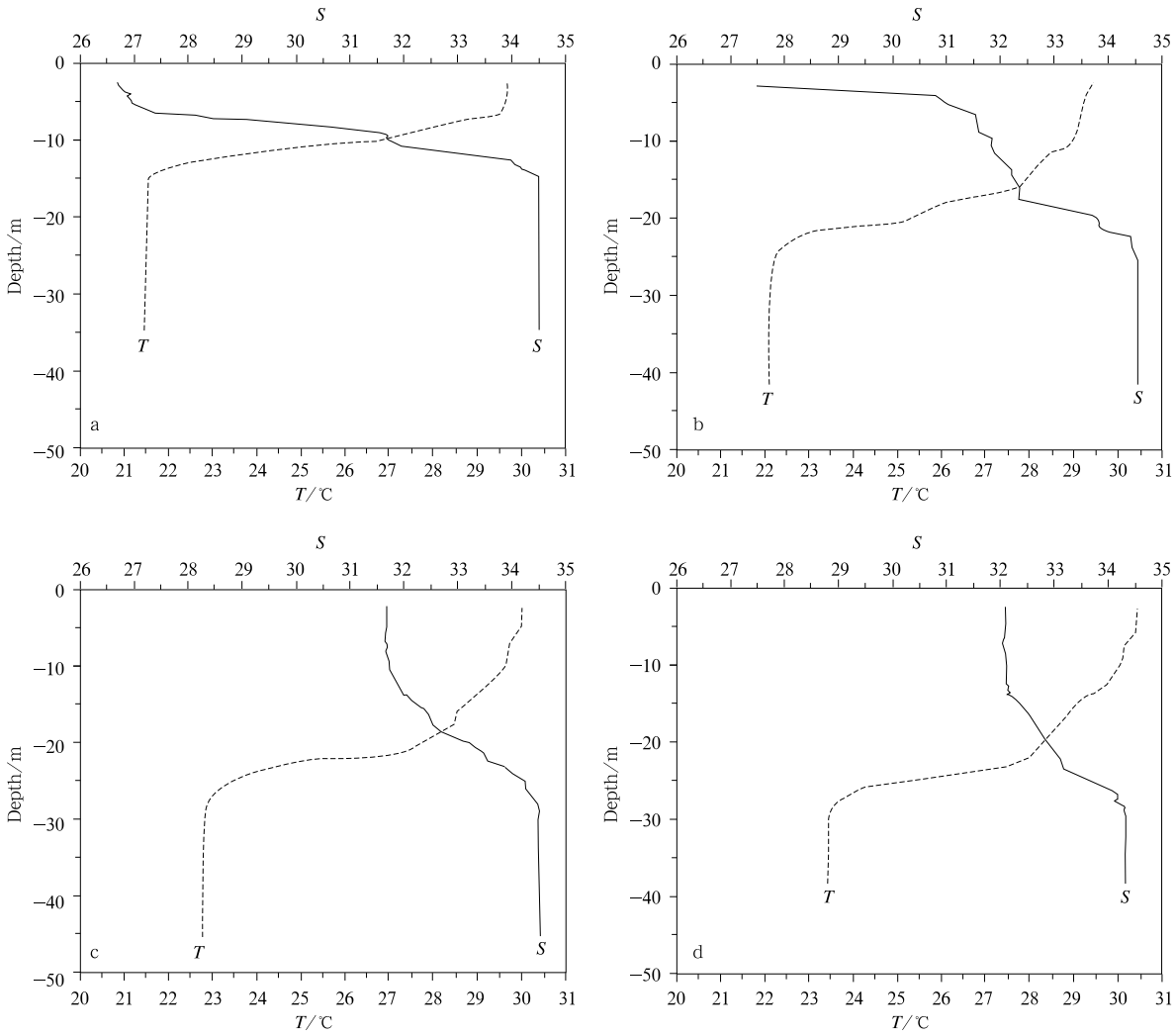

Fig.2. Vertical profiles of temperature (T, dashed line) and salinity (S, solid line) measured by CTD cast at Stas E1 (a), E2 (b), E3 (c) and E4 (d).

parallel to the direction of coastlines at an offshore distance of about 60 km. Defining 32 isohaline as the boundary of the low salinity tongue (Wu, 1989), a maximum width of the tongue at the surface layer (depth of 5 m) reaches 70 km. The low salinity tongue tip reaches 23.2°N, 118.3°E. The low salinity tongue root is located on the southwest side of the study area, where the lowest salinity is only 27, implying that the low salinity water originated from somewhere southwest of the survey area.

Vertically, at the 10 m layer, the low salinity tongue keeps the patterns similar to that at the surface layer. The location of low salinity tongue tip keeps unchanged, but the width narrows to a maximum of about 45 km at the water tongue root. The lowest salinity increases 2.5 to 29.5. The low salinity water exists even at the near-bottom layer (30 m), but cannot keep an entire tongue pattern below the 15 m layer. In other words, the low salinity water is mainly concentrated in the upper layer from the sea surface to about 10 m depth.

Horizontally, from Figs 3a–e, the salinity gradients can be calculated. Taking Fig. 3b (10 m layer) as an example, along the west boundary of survey area, the salinity gradients reach 0.24 km^{-1} on the shallow water side, and 0.085 km^{-1} along the east boundary of the study area on the deep water side, respectively. This implies the existence of strong salinity fronts on both sides of the low salinity tongue according to a generally accepted criterion of 0.018 km^{-1} for a salinity front (Zhuang et al., 2003). Meanwhile, the existence of strong salinity fronts implies that a jet-like current has to serve as a low salinity water supplier to maintain the existence of low salinity tongue

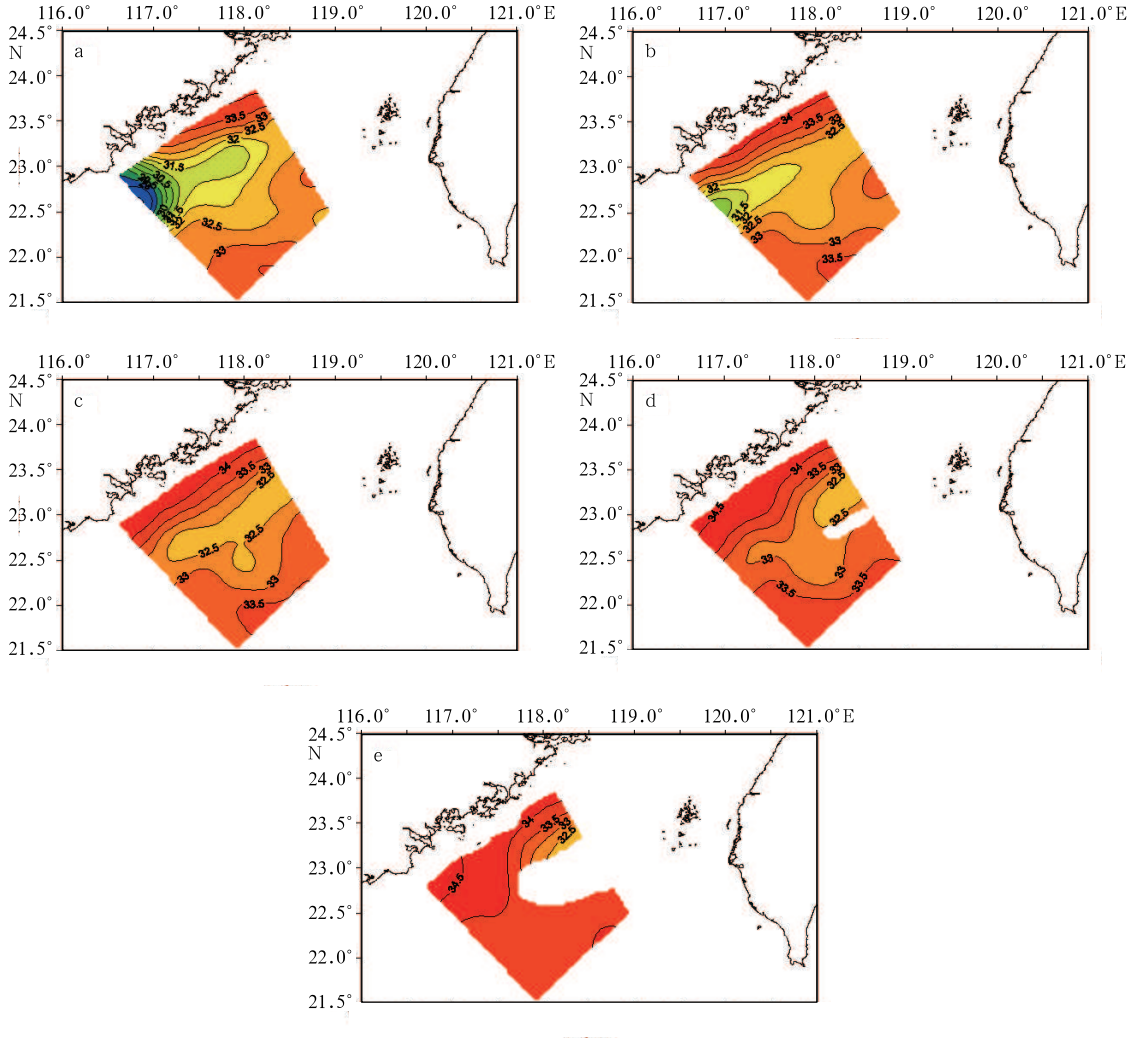

Fig.3. 2-D distribution maps of the salinity at depths of 5 m (a), 10 m (b), 15 m (c), 20 m (d), and 30 m (e) derived from the cruise data of the summer of 2005 and interpolation methods.

(Zheng et al., 2004).

2-D distribution maps of the water temperature at depths of 5, 10, 15, 20, and 30 m derived from the cruise data of the summer of 2005 and interpolation methods are shown in Figs 4a–e. One can see that the temperature in the low salinity tongue is much higher than that in the coastal water and the same as that in the deep water. At the surface layer (Fig. 4a), the temperature in the low salinity water tongue ranges from 29 to 30°C, at least 6°C higher than that at the coastal water. At the near-bottom layer, the temperature varies from 24 to 28°C, at least 3°C higher than that at the coastal water. Between the low salinity tongue and the coastal water, there is a strong temperature front. At the surface layer, the temperature gradient across the front reaches 0.24°C/km, four times higher than a generally accepted criterion of 0.054°C/km for a temperature front (Zhuang et al., 2003). While on the deep water side, there is not a temperature front existing up to 15 m. Only at the near-bottom layer, a temperature front can be observed. According to the previous results, the low temperature and high salinity coastal waters are generated by summer monsoon-induced coastal upwelling (Hu et al., 2003; Hu et al., 2001b), and the high temperature and high salinity water on the deep water side of the low salinity tongue is transported by the SCS Warm Current from the northern SCS (Li et al., 2000; Guan and Fang, 2006).

4 Verification by numerical modeling

The analysis of 2-D maps of low salinity tongue has revealed that the low salinity water should origi-

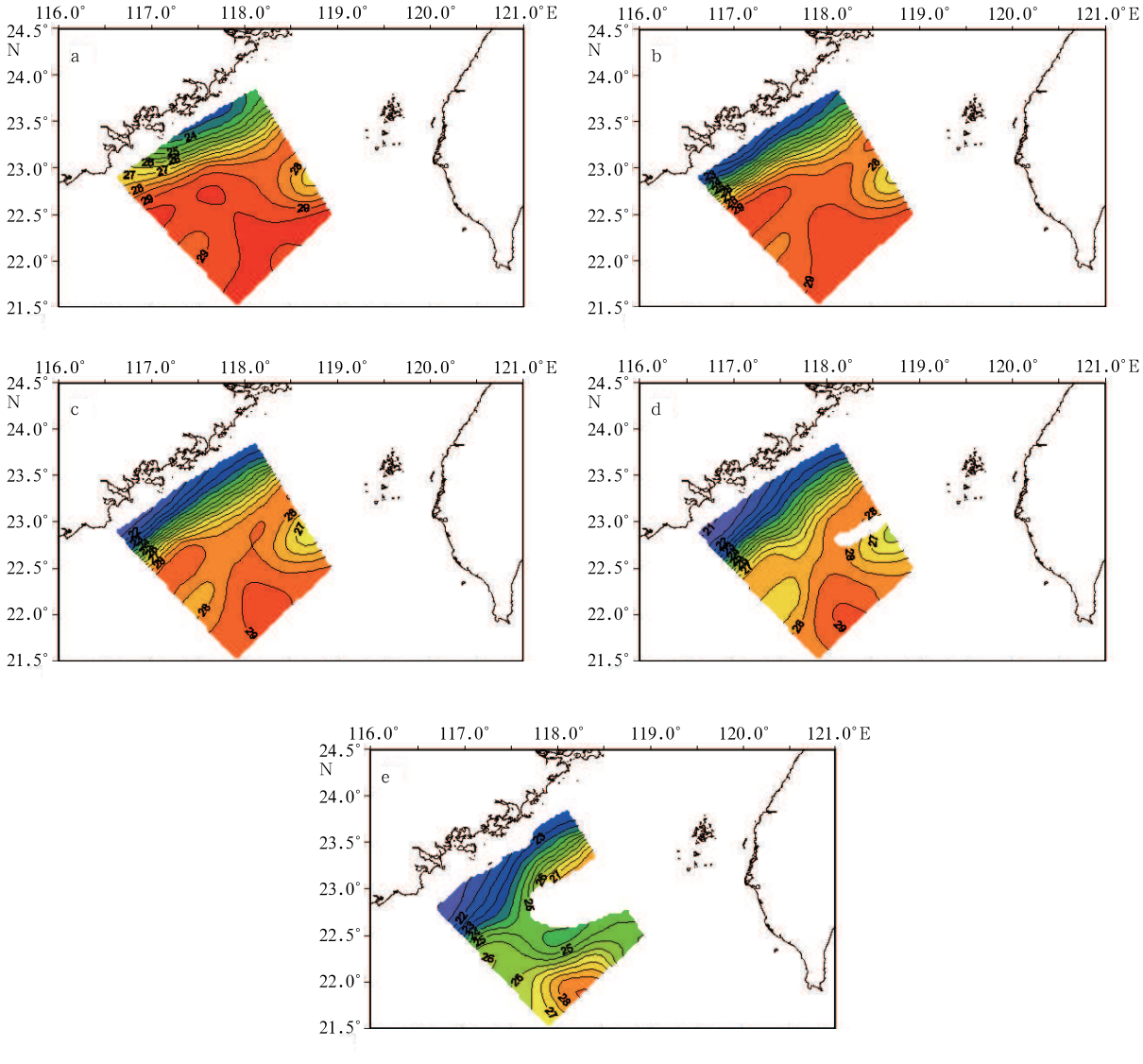

Fig.4. 2-D distribution maps of water temperature (°C) at depths of 5 m (a), 10 m (b), 15 m (c), 20 m (d), and 30 m (e) derived from the cruise data of the summer of 2005 and interpolation methods.

nate from somewhere southwest of the study area. Calculations indicate that diluting the water volume contained in the low salinity tongue from 34.5 to an average salinity of 29.5 needs 9×10^9 m^3 of fresh water. This amount needs a huge fresh water supplier. Checking the rivers nearby, the nearest one is the Hanjiang River with an annual runoff of 2.6×10^{10} m^3 (Chen and Zhao, 1985). This means that 4.15 months of the Hanjiang River runoff is needed to form the low salinity tongue. Clearly, this supplier is too slow. The other potential fresh water supplier is the Zhujiang (Pearl) River, which is located at about 300 km upstream from the west boundary of the study area. Its annual runoff reaches 3.6×10^{11} m^3 (Chen and Zhao, 1985; Chen and Wang, 2004). To form the low salinity tongue needs 0.3 month of its runoff, implying that the Zhujiang River is a qualified fresh water supplier. Thus, we judge that the tongue-like high temperature and low salinity water is originated mainly from the Zhujiang Estuary. This judgment has been verified by the following numerical modeling results.

A numerical model was developed from the Princeton ocean model (Blumberg and Mellor, 1987). A nest strategy was used, in which the coarse-grid domain covered the northwestern Pacific with 1/5 degree grid and the fine-grid domain covered the Taiwan Strait and its adjacent area with 1/25 degree grid. In the vertical direction, there were 21 sigma levels. The fluxes at the sea-air interface were downloaded from the National Center for Environmental Predic-

tion (Kalnay et al., 1996), the monthly climatological thermohaline parameters along the open boundaries came from a Pacific regional ocean model system (PROMS, Liu and Chai, 2009), and monthly mean runoff was set for each river along the coast of China. The details of construction and verification of the model were given by Jiang (2007). Figure 5 shows one example of numerical modeling results of salinity distribution at 5 m in the survey area during the cruise period. One can see a low salinity tongue originating from the Zhujiang River Estuary extends all the way to the Taiwan Strait. Evidently, the Zhujiang River Estuary serves as a main water source of the low salinity water. These results agree quite well with the cruise measurements, implying that the low salinity tongue indeed exists and its upstream can be traced back to the Zhujiang River Estuary. Another model result from Gan et al. (2009) also indicates that the plume from the Zhujiang River can extend northeastward to the southern Taiwan Strait.

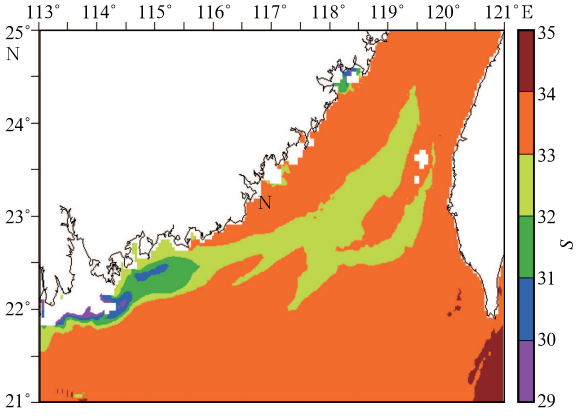

Fig.5. Numerical modeling result of salinity distribution at 5 m in the study area during the cruise measurements.

5 Summary and discussion

Cruise CTD observations in the summer of 2005 reveal that a low salinity tongue intrudes the Taiwan Strait. The water body of the low salinity tongue is characterized by the high temperature and low salinity, with the temperature 3–6°C higher than that of the coastal water and the salinity 2.5–7.0 lower than that at the surrounding waters, in the upper layer from the surface to a depth of 10 m. These features imply a nature of river diluted water of the low salinity tongue (Zhuang, 2003; Wu, 1989). The numerical modeling results show that a low salinity tongue originating from the Zhujiang River Estuary extends all the way to the Taiwan Strait, suggesting that the low salinity tongue indeed exists and its upstream can be traced back to the Zhujiang River Estuary.

The data analysis indicates that a current is needed to carry the low salinity water to the study area and to maintain the existence of strong salinity fronts on both sides of low salinity tongue. Considering the monsoon climate in the study area, we judge that this jet-like current should have a nature of monsoon drift (Fu and Hu, 1995). Meanwhile, the coastal upwelling from the left hand side and the SCS Warm Current from the right hand side confine the low salinity water to flow along the central line of the strait and to form a jet-like pattern. Thus, it is reasonable to say that the low salinity tongue is produced by four major elements: river diluted water, monsoon wind driving, coastal upwelling and SCS Warm Current modifications.

The intrusion of the Zhujiang River diluted water into the Taiwan Strait is an important concept for the local circulation study. In fact, the previous investigators have pointed out that the low salinity diluted water spreads eastward from the Zhujiang River Estuary (Gan et al., 2009; Zhuang et al., 2003; 2005). This point was evidenced by the field measurements of the cruise in the summer of 2000 (Zhuang et al., 2003). The contribution of this study provides new evidence to this important conclusion and further finding out that the north tip of the diluted water may reach as far as to the central Taiwan Strait. Thus, for future cruise measurements and modeling, it is significant to determine its seasonal variability and interannual variability.

Zhuang et al. (2003) and Li et al. (2000) pointed out that the diluted water from the Hanjiang River Estuary may also spread into the southern Taiwan Strait and the Taiwan Bank area. The location of the Hanjiang River Estuary is much closer to the study area than the Zhujiang River Estuary, and the peak phase of its runoff is concentrated in summer. Therefore, the contribution of the diluted water from the Hanjiang River Estuary to the observed low salinity tongue should also be counted in the analysis and the future modeling, although its annual runoff is much smaller than the Zhujiang River.

Acknowledgements

The authors thank the crew of R/V *Yanping No. 2* for their help in the field work. The authors are much obliged to the editors and anonymous reviewers for their useful comments which enabled the authors

to improve the manuscript a great deal.

References

Bao X, Hou Y, Chen C, et al. 2005. Analysis of characteristics and mechanism of current system on the west coast of Guangdong of China in summer. Acta Oceanologica Sinica, 24(4): 1–9

Blumberg A F, Mellor G L. 1987. A description of a three-dimensional coastal ocean circulation model. In: Heaps N, ed. Three-Dimensional Coastal Ocean Models, Coastal Estuarine Stud., v4. Washington, D C: AGU, 1-16

Chen X. 1983. On the distribution of the tidal current in the Taiwan Strait. Marine Sci Bull, 2: 16–24

Chen Z, Hu J, Huang B, et al. 2005. Temperature and Salinity Data Report: Cruise in the Southwestern Taiwan Strait during July 2005, Technical Report: No. CMI-001. Xiamen: Xiamen Univ, 1–200

Chen Z, Hu J, Zhang C, et al. 1999. The characteristics of tidal current and residual current in the southern Taiwan Strait in August, 1997. J Xiamen Univ (Natural Science), 38(2): 268–272

Chen J, Wong L. 2004. Methodology for estimation of river discharge and application of the Zhujiang River Estuary (ZRE). Acta Oceanologica Sinica, 23(3): 377–386

Chen T, Zhao C. 1985. Water and sand discharges of China major rivers and their influence on coasts. Acta Oceanologica Sinica(in Chinese), 7: 460–471

Chuang W S. 1986. A note on the driving mechanism of the current in the Taiwan Strait. J Oceanogr Soc, 42: 355–361

Ding L. 1983. Tides and characteristics of the tidal currents in the Taiwan Strait. Taiwan Strait, 2: 1–8

Fu Z, Hu J. 1995. Current structures and seawater volume flux through Taiwan Strait. Tropic Oceanol, 14: 75–80

Gan J, Li L, Wang D, et al. 2009. Interaction of a river plume with coastal upwelling in the northeastern South China Sea. Continental Shelf Research, 29(4): 728–740

Guan B, Fang G. 2006. Winter counter-wind currents off the southeastern China coast: a review. J Oceanogr, 62: 1–24

He Z, Wang D, Hu J. 2002. Features of eddy kinetic energy and variations of upper circulation in the South China Sea. Acta Oceanologica Sinica, 21(2): 305–314

Hu J, Kawamura H, Hong H, et al. 2001a. 3–6 months variation of sea surface height in the South China Sea and its adjacent ocean. J Oceanogr, 57: 69–78

Hu J, Kawamura H, Hong H, et al. 2001b. Hydrographic and satellite observations of summertime upwelling in the Taiwan Strait: a preliminary description. TAO, 12: 415–430

Hu J, Kawamura H, Hong H, et al. 2003. A review of research on the upwelling in the Taiwan Strait. Bull Marine Sci, 73: 605–628

Hu J, Liang H, Zhang X. 1999. Distributional features of temperature and salinity in southern Taiwan Strait and its adjacent sea areas in late summer, 1994. Acta Oceanologica Sinica, 18(2): 237–246

Jan S, Chern C-S, Wang J, et al. 2004. The anomalous amplification of M_2 tide in the Taiwan Strait. Geophys Res Lett, 31: L07308, doi:10.1029/2003GL019373

Jiang Y W. 2007. The now-cast system for the current of the Taiwan Strait: a study of three-dimensional numerical model. Technical Report. State Key Laboratory of Marine Environmental Science, Xiamen University, Xiamen, Fujian, China

Kalnay E, Kanamitsu M, Kistler R, et al. 1996. The NCEP/NCAR 40-year reanalysis project. Bulletin of the American Meteorological Society, 77: 437–471

Kuo N-J, Ho C-R. 2004. ENSO effect on the sea surface wind and sea surface temperature in the Taiwan Strait. Geophys Res Lett, 31: L13309, doi: 10.1029/2004GL020303

Li L, Guo X, Wu R. 2000. Oceanic fronts in southern Taiwan Strait. J Oceanogr Taiwan Strait, 19: 147–156

Li L, Nowlin W D Jr, Su J. 1998. Anticyclonic rings from Kuroshio in the South China Sea. Deep-Sea Res (I), 45: 1469–1482

Liu G, Chai F. 2009. Seasonal and interannual variability of primary and export production in the South China Sea: a three-dimensional physical-biogeochemical modeling study. Journal of Marine Sciences, 62(2): 420–431

Liu Y, Yuan Y. 1999. Variability of the Kuroshio in the East China Sea in 1993 and 1994. Acta Oceanologica Sinica, 18(1): 17–36

Wu B. 1989. A study on the circulation in shelf waters west to Zhujiang Estuary: I. Coastal current. J Oceanogr Taiwan Strait, 8: 360–365

Zheng Q, Clemente-Colón P, Yan X-H, et al. 2004. Satellite SAR detection of Delaware Bay plumes: jet-like feature analysis. J Geophys Res, 109: C03031, 10.1029/2003JC002100

Zheng Q, Klemas V. 1982. Determination of winter temperature patterns, fronts, surface currents in the Yellow Sea and East China Sea from satellite imagery. Rem Sens Environ, 12: 201–218

Zhuang W, Hu J, He Z, et al. 2003. An analysis on surface temperature and salinity from southern Taiwan Strait to Zhujiang River Estuary during July–August, 2000. J Tropical Oceanog., 22: 68–76

Zhuang W, Wang D, Wu R, et al. 2005. Coastal upwelling off eastern Fujian–Guangdong detected by remote sensing. Chin J Atmos Sci, 29: 438–444